Original Article

Amygdalin attenuates PM2.5-induced human umbilical vein endothelial cell injury via the TLR4/NF-κB and Bcl-2/Bax signaling pathways

Bixu Wang[1], Tong Sun[1], Ling Sun[1], Lan Li[2], Haitong Wan[2], Zhishan Ding[1], and Xiaoqing Ye[1,*]

[1]School of Medical Technology and Information Engineering, Zhejiang Chinese Medical University, Hangzhou 310053, China, and [2]School of Life Sciences, Zhejiang Chinese Medical University, Hangzhou 310053, China
*Correspondence address. +86-571-86633307; E-mail: yexq@zcmu.edu.cn

Abstract

Mounting evidence supports that long-term exposure to fine particle pollutants (PM2.5) is closely implicated in cardiovascular diseases, especially atherosclerosis. Amygdalin is reported to attenuate external stimuli-induced cardiovascular diseases. However, the underlying mechanisms are still not understood. In this study, we aim to explore the protective effects of amygdalin on PM2.5-induced human umbilical vein endothelial cell (HUVEC) injury and unravel the specific mechanisms by MTT, DCFH-DA, biochemical, immunofluorescence, ELISA, RT-qPCR, flow cytometry, TUNEL and western blot analysis. The results reveal that amygdalin reverses PM2.5-induced cytotoxicity and attenuates intracellular ROS production. Moreover, amygdalin increases the levels of SOD and GSH and alleviates the MDA content. Additionally, amygdalin causes a decline of IL-6, IL-1β, TNF-α and COX-2 levels. Moreover, amygdalin inhibits NF-κB p50 and TLR4 protein expressions and NF-κB p65 nuclear translocation. Concomitantly, a decline of phospho-NF-κB p65/NF-κB p65 and phospho-IκB-α/IκB-α is detected. Meanwhile, amygdalin pretreatment reduces HUVEC apoptosis. In addition, amygdalin triggers an upregulation of Bcl-2 and a downregulation of Bax after stimulation with PM2.5. Collectively, these results suggest that amygdalin suppresses PM2.5-induced HUVEC injury by regulating the TLR4/NF-κB and Bcl-2/Bax signaling pathways, indicating that amygdalin may be a novel target for atherosclerosis treatments.

Key words amygdalin, PM2.5, inflammation, oxidative stress, apoptosis

Introduction

Air pollution is gradually becoming severe all over the world due to the improvement of life quality and the rapid development of industry. The World Health Organization Air Quality Guidelines recommended PM2.5, the particulate matter with an aerodynamic equivalent diameter less than or equal to 2.5 microns, as an indicator for air pollution. PM2.5, which has been regarded as one of the most harmful factors to human health, is increasingly becoming a public concern around the world because it has complex composition and is difficult to be metabolized by the whole body [1]. A number of studies have elaborated that PM2.5 exposure increases the morbidity and mortality of many diseases, including neurodegenerative diseases, airway damages, cardiovascular im-

pairments and diabetes mellitus [2,3]. Moreover, *in vivo* and *in vitro* experiments have illustrated that real-ambient PM2.5 exposure induces injuries and systemic damages to multiple organs, including the cardiovascular system, internal digestive system, reproductive system and respiratory system, among which the cardiovascular system is most likely to be affected [4–7]. Additionally, epidemiological studies also showed that long-term PM2.5 exposure is closely associated with cardiovascular disease (CVD) [8,9]. It is well known that atherosclerosis (AS) is the pathological basis of CVD, and the burden of AS has markedly increased in China, especially with aging. Epidemiological evidence showed that approximately 2.4 million people died from AS in 2016, accounting for 61% of deaths from CVD and 25% of total deaths

[10]. Although the mechanisms of AS caused by PM2.5 exposure are still unclear, increasing evidence indicates that inflammation, oxidative stress and apoptosis are related to it. Since heavy metal substance-containing PM2.5 accumulates instead of being biodegraded in the body, it can cause ROS-mediated cell toxicity [11]. It was reported that PM2.5 could induce systemic inflammation and endothelial cell (EC) dysfunction, resulting in destabilization of atherosclerotic plaques [12–14]. Moreover, several studies have shown that PM2.5 can impair mitochondrial membrane structure, induce oxidative stress, and activate the apoptosis pathway [1,15,16]. Therefore, there is an urgent need for preventive and therapeutic measures targeting AS.

PM2.5 can penetrate the blood-brain and air-blood barriers, triggering AS. It is known that EC dysfunction is the initiating link in the early period of AS, resulting in foam cell development and plaque maturation [17]. Additionally, endovascular therapy is widely used in the treatment of CVD [7]. Vein endothelial cells play an important role in resisting external stimuli in the body; thus, human umbilical vein endothelial cells (HUVECs) are usually used to establish AS models *in vitro*. Inflammation is the initial response to eliminate cell damages, and it has been shown that HUVECs exposed to PM2.5 induce the overexpressions of interleukin-6 (IL-6) and tumor necrosis factor-α (TNF-α), which are significant cytokines in inflammatory and immune responses [13]. Furthermore, a previous *in vitro* study demonstrated that PM2.5 could enter ECs, induce excessive expression levels of reactive oxygen species (ROS), and further trigger oxidative stress [18]. Antioxidants, such as superoxide dismutase (SOD), glutathione (GSH), and glutathione peroxidase (GSH-Px), and peroxidation products, such as malondialdehyde (MDA), play essential roles in balancing oxidation and antioxidation reactions [19]. It was illustrated that PM2.5 exposure could result in downregulation of SOD activity and GSH levels and upregulation of MDA contents [20]. Toll-like receptors (TLRs) are important proteins involved in natural molecular immunity, and TLR4 is the most studied receptor [21]. Several studies have demonstrated that the TLR4/NF-κB signaling pathway participates in the occurrence and development of CVD [22,23]. Bcl-2 and Bax are key molecules that take part in the senescence of endothelial cells (ECs) [24–26]. Therefore, determination of the molecular mechanisms of EC injury and dysfunction could provide novel approaches to prevent and treat AS.

In recent years, an increasing number of researchers have been devoted to exploring the therapeutic potentials and mechanisms of traditional Chinese medicine ingredients, owing to their safety and great curative effects. Amygdalin, a β-type glycoside, is an ingredient from *Prunus persica* (L.) Batsch. It has been demonstrated that amygdalin has the potential to treat liver cancer by inducing mitochondria-mediated autophagy and apoptosis [27]. Furthermore, amygdalin inhibits the growth of prostate cancer cells by delaying cell cycle progression and inducing the apoptosis of Hs578T triple-negative breast cancer cells and HepG2 cells [28,29]. In addition to inhibiting the growth of tumor cells, amygdalin can also be used to treat fibrosis. Evidence *in vivo* and *in vitro* has demonstrated that amygdalin treatment attenuates TFG-β1-induced hepatic stellate cell (HSC) activation and CCl₄-stimulated rat hepatic fibrosis [30]. Another study showed significant anti-inflammatory and anti-apoptotic effects of amygdalin in LPS-treated BEAS-2B bronchial epithelial cells [31]. Moreover, amygdalin attenuates inflammatory and oxidative responses by downregulating the levels of cyclooxygenase-2 (COX-2), TNF-α and phosphorylated-NF-κB (p-NF-κB) and upregulating the protein expressions of SOD-2, GPX-4 and Nrf2 [32]. Additionally, amygdalin suppresses inflammation and apoptosis via the NF-κB, MAPK, and AP-1 signaling pathways in ox-LDL-stimulated bone marrow-derived macrophages and ApoE$^{-/-}$ mice [33]. However, to our knowledge, the protective effects and mechanisms of amygdalin on HUVECs exposed to PM2.5 have not been clarified.

In the present study, we aimed to determine whether amygdalin protects against PM2.5-induced HUVEC injury through the TLR4/NF-κB and Bcl-2/Bax signaling pathways and elucidate the potential mechanisms of the protective effects of amygdalin on AS.

Materials and Methods
Amygdalin preparation
Amygdalin (≥98% purity by high-performance liquid chromatography, CAS No: 29883-15-6, Lot. No. Z28A6L2815) was purchased from Shanghai Yuanye Bio-Technology Co., Ltd (Shanghai, China). A stock solutions (2 mg/mL) was prepared by dissolving it in Roswell Park Memorial Institute-1640 (RPMI-1640; Gibco, Carlsbad, USA), and diluted to the required concentration for further experiments.

PM2.5 sample collection, preparation and composition analysis
The collection and extraction of PM2.5 were performed as described in a previous article by our laboratory [27]. Briefly, PM2.5 samples were continuously collected from August 2017 to November 2017 at Zhejiang Chinese Medical University (E 120° 9′ 16″, N 30° 11′ 1″) with a Thermo Anderson G-2.5 large-volume sampler (1.13 m³/min; Thermo Fisher Scientific, Waltham, USA). The sampler was placed on the roof of Building No. 4, approximately 20 meters away from the ground. The PM2.5 samples were collected on glass quartz-fibre filters (203 mm × 254 mm; Thermo Fisher Scientific), which were prebaked at 300°C for 5 h before use. All glass fiber filters were cut into small pieces (0.5 cm × 0.5 cm) and immersed in ultrapure water under sterile conditions. Then, the samplers were eluted for 12 h at 200 rpm in a shaker and sonicated at 80 Hz five times (30 min each time). The extracted liquid was filtered with eight layers of sterile gauze and vacuum freeze-dried. The PM2.5 samples were weighed, resuspended in RPMI-1640, sonicated for 30 min and vortexed prior to use. The concentrations of elements were determined with an inductively coupled plasma mass spectrometer (ICP-MS, Thermo X series; Thermo Fisher Scientific) and a 7890A-5975C gas chromatography-mass spectrometer equipped with an electron ionization ion source (GC-MS; Agilent Technologies, Santa Clara, USA). All processes were carried out under dark conditions.

Cell culture
The HUVEC line was purchased from the China Center for Type Culture (CCTCC, Wuhan, China). HUVECs were cultured in RPMI-1640 supplemented with 10% fetal bovine serum (FBS; Gibco) and 1% penicillin-streptomycin antibiotic (Genom, Hangzhou, China) at 37°C in a humidified atmosphere of 5% CO₂ and subcultured periodically.

Cell viability analysis
To investigate the cytotoxicity of PM2.5 and amygdalin, HUVECs

were treated with different concentrations of PM2.5 or amygdalin for 24 h. Cell viability was measured by 3-(4,5-dimethylthiazol-2-yl)-2,5-diphenyl tetrazolium bromide (MTT) asssy. Briefly, HUVECs were trypsinized at approximately 80% confluence, and 100 μL of cell suspension was seeded in 96-well plates at a final concentration of 5×10^3 cells/well. After overnight adherence, cells in each well were treated with PM2.5 (0, 25, 50, 100, 200 and 400 μg/mL) or amygdalin (0, 2.5, 5, 10, 20, 40, and 100 μg/mL) for 24 h. Then, 20 μL MTT (5 mg/mL; Sangon Biotech, Shanghai, China) was added to each well, followed by incubation at 37°C for 4 h in the dark. Finally, blue-violet crystals in each well were dissolved in DMSO, and the absorbance of each well was detected at 570 nm with an Epoch2™ microplate spectrophotometer (BioTek, Winooski, USA). The experiments were conducted in triplicate with nine replicate wells each time.

ROS measurement

Reactive oxygen species (ROS) generation in HUVECs was detected by the dichlorofluorescein-diacetate assay (DCFH-DA). HUVECs were pretreated with or without amygdalin (2.5, 5, and 10 μg/mL) for 2 h before stimulation with PM2.5 (100 μg/mL) for 24 h. Then, HUVECs were washed with PBS and incubated with 10 μM DCFH-DA (Beyotime Biotechnology, Shanghai, China) for 20 min at 37°C in the dark. After being washed three times, the cells were examined under an epifluorescence microscope (Eclipse Ti-Dh; Nikon, Tokyo, Japan), and the fluorescence intensity was analyzed with ImageJ software.

Oxidation product assay

The activity of superoxide dismutase (SOD) and the contents of malondialdehyde (MDA) and glutathione (GSH) were determined using a Superoxide Dismutase Assay kit, lipid peroxidation MDA assay kit, and total glutathione assay kit (Beyotime Biotechnology), respectively according to the manufacturer's protocols.

Inflammatory cytokine assay

HUVECs were pretreated with amygdalin (2.5, 5, and 10 μg/mL) for 2 h, followed by stimulation with PM2.5 (100 μg/mL) for 24 h. The culture medium in each group was centrifuged at 1000 g for 15 min at 4°C to obtain the supernatants. IL-6, TNF-α and IL-1β levels in the supernatant were measured using the corresponding enzyme-linked immunosorbent assay kit (ELISA; Meimian, Nanjing, China) according to the manufacturer's instructions. The absorbance of each well was analyzed with an Epoch2 microplate spectrophotometer (BioTek). Finally, the levels of TNF-α, IL-6 and IL-1β were calculated through the standard curves.

Quantitative real-time PCR assay

HUVECs were preincubated with amygdalin (2.5, 5, and 10 μg/mL) for 2 h followed by stimulation with PM2.5 (100 μg/mL) for 24 h. An RNA-Quik Purrification kit (Yishan Biotech, Shanghai, China) was used to extract total RNA from the cells as described in the manufacturer's instructions. The concentration and purity of total RNA were quantified with a microultraviolet-visible spectrophotometer (Thermo Fisher Scientific). PrimeScript RT reagent kit with a gDNA Eraser (Takara Biotechnology, Kyoto, Japan) was used to reverse transcribe the total RNA into cDNA. The expression of cDNA was assessed by real-time PCR using TB Green Premix Ex Tap II Tli RNaseH Plus (Takara Biotechnology) on an ABI-7500 Real-Time PCR System (Foster City, USA). The $2^{-\triangle\triangle Ct}$ method was used to calculate the relative expression levels of *IL-6*, *TNF-α*, *IL-1β* and *COX-2*. *β-Actin* was used as the internal reference control. The sequences of different primers are listed in Table 1.

Immunofluorescence analysis

After pretreatment, HUVECs in each group were washed three times with PBS, fixed with immunol staining fix solution (Beyotime Biotechnology) and permeabilized with Triton X-100 (Beyotime Biotechnology). The nonspecific protein binding sites were blocked with immunol staining blocking buffer (Beyotime Biotechnology). The above steps were performed at room temperature for 20 min. Then, samples were incubated with primary antibody against NF-κB p65 (1:200; Cell Signaling Technology, Beverly, USA) for 2 h and incubated with an Alexa Fluor 488-labelled secondary antibody (1:200; Abcam, Cambridge, UK). Then, the HUVEC nuclei were stained with 4',6-diamidino-2-phenylindole (DAPI) for 5 min. The location and fluorescence intensity of NF-κB p65 were visualized with a laser scanning confocal microscope (Zeiss, Oberkochen, Germany).

Western blot analysis

Protein expression levels related to the TLR4/NF-κB signaling pathway and Bcl-2/Bax signaling pathway were quantified by western blot analysis. After different treatments, HUVECs in each well were lysed on ice using radio immunoprecipitation assay buffer (RIPA; Beyotime Biotechnology) containing phenylmethanesulfonyl fluoride (PMSF; Cell Signaling Technology) and 100 × Phosphatase inhibitor complex I (Sangon Biotechnology). Total protein concentrations were measured using the bicinchoninic acid protein assay reagent (Takara Biotechnology). Equal amounts of protein in each group were separated by SDS-PAGE and transferred to polyvinylidene fluoride membranes (Millipore, Billerica, USA). After being blocked with 5% bovine serum albumin (BSA; Amresco, Radnor, USA) for 2 h, the membranes were incubated with primary antibodies against β-actin (1:5000), TLR4 (1:1000; Santa Cruz Biotechnology, Santa Clara, USA), COX-2, NF-κB p65, p-NF-κB p65, NF-κB p50, IκB-α, p-IκB-α, Bcl-2 and Bax (1:1000; Cell Signaling Technology) at 4°C overnight. Then, HRP-conjugated secondary antibodies against rabbit or mouse IgG were incubated with the membranes for 2 h at room temperature. Finally, enhanced chemiluminescence substrate (PerkinElmer, Wellesley, USA) was added to the membranes, and the protein bands were detected with a chemiluminescence imaging system (Tanon, Shanghai, China).

Table 1. Sequences of primers used for quantitative real-time PCR

Gene	Primer sequence (5′→3′)
COX-2	Forward: CTGTATCCCGCCCTGCTGGTG
	Reverse: ACTTGCGTTGATGGTGGCTGT
IL-6	Forward: TTCTCCACAAGCGCCTTCGGTCCA
	Reverse: AGGGCTGAGATGCCGTCGAGGATGTA
TNF-α	Forward: TCTGGGCAGGTCTACTTTGG
	Reverse: GGTTGAGGGTGTCTGAAGGA
IL-1β	Forward: GCATCCAGCTACGAATCTCC
	Reverse: CCACATTCAGCACAGGACTC
β-Actin	Forward: ATCATGTTTGAGACCTTCAACA
	Reverse: CATCTCTTGCTCGAAGTCCA

The band intensities were quantified with ImageJ software.

Apoptosis analysis

Annexin V-FITC/PI Apoptosis Detection kit (BD Biosciences, Franklin Lakes, USA) was used to measure cell apoptosis. Briefly, HUVECs in 12-well plates were resuspended in 500 μL binding buffer and stained with 10 μL PI and 10 μL FITC. After incubation in the dark for 15 min, cell apoptosis was detected by flow cytometry on the BD Accuri C6 flow cytometer (BD Biosciences).

TUNEL staining assay

The apoptosis of HUVECs was also assessed using a TUNEL assay kit (Beyotime Biotechnology) according to the manufacturer's protocol. The HUVECs were stained with DAPI for 5 min and images were captured with an epifluorescence microscope.

Statistical analysis

All experiments were repeated three times. Bar graphs were generated using GraphPad Prism 5.0. Data analysis was performed using SPSS 17.0 software and presented as the mean ± SD. Statistical evaluation was performed by one-way analysis of variance (ANOVA) followed by post hoc Tukey's test. $P < 0.05$ was regarded as statistically significant.

Results

The composition of PM2.5

Due to the complexity of the source and composition of PM2.5, it has endangered human life in recent years [4–6]. In our previous study [34], the concentrations of metals and polycyclicaromatichydrocarbons (PAHs) in PM2.5 were evaluated by ICP-MS and EI-MS, respectively. The results showed that PM2.5 contained high concentrations of potassium, sodium, calcium, magnesium and zinc. Meanwhile, PM2.5 adsorbed many toxic heavy metals, such as nickel, lead, chromium, zinc, cadmium and thallium, due to the dust of increasing constructions and roads. From PAH analysis, we found that the most abundant PM2.5 is benzo(b,j)fluoranthene. In addition, chrysene, fluoranthene, perylene, benzo(a)pyrene, benzo(c)phenanthrene and benzo(e)pyrene were also detected at high concentrations in PM2.5, which may be due to pollution from the chemical industry and transportation in Hangzhou, China.

Amygdalin reduced the cytotoxicity of PM2.5 to HUVECs and inhibited PM2.5-induced ROS production in HUVECs

The viability of HUVECs exposed to PM2.5 and amygdalin was measured by MTT assay. As shown in Figure 1A, PM2.5 exhibited remarkable cytotoxicity at concentrations greater than 50 μg/mL ($P < 0.05$ or $P < 0.01$). When the cells were incubated with PM2.5 at 100 μg/mL for 24 h, the cell viability was approximately 75%, which was the optimal concentration for further experiments as reported [3]. Figure 1B showed that incubation with 0–100 μg/mL amygdalin was nontoxic to HUVECs. In addition, pretreatment with 2.5–100 μg/mL amygdalin for 2 h in the presence of 100 μg/mL PM2.5 for 24 h abolished the cytotoxicity of PM2.5 to HUVECs (Figure 1C).

The abnormal increase in reactive oxygen species (ROS) is one of the key indicators in response to PM2.5 stimulation in HUVECs. As shown by the DCFH-DA fluorescence intensity results, PM2.5 exposure significantly increased ROS levels (Figure 1D). However, with pretreatment with amygdalin for 2 h followed by stimulation with PM2.5 for 24 h, the green fluorescence intensities were lower than those in the PM2.5 group. Moreover, ROS production was
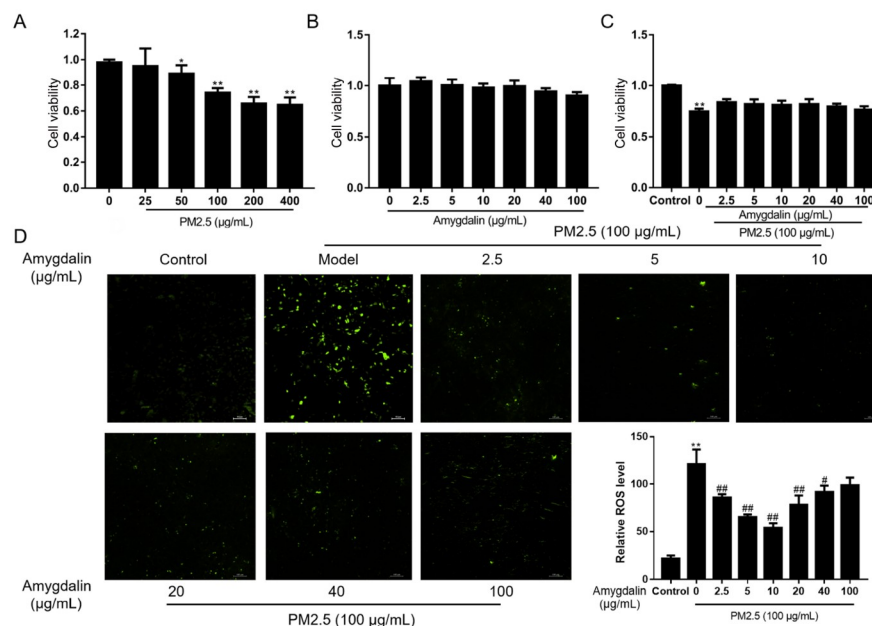

Figure 1. Cytotoxicity of PM2.5 and amygdalin and determination of ROS production in HUVECs (A) Cell viability of HUVECs treated with different concentrations of PM2.5 for 24 h. (B) Cell viability of HUVECs treated with different concentrations of amygdalin for 24 h. (C) Cell viability of HUVECs pretreated with different concentrations of amygdalin for 2 h, followed by treatment with 100 μg/mL PM2.5 for 24 h. (D) ROS production after pretreatment with different concentrations of amygdalin, followed by treatment with 100 μg/mL PM2.5 for 24 h, was measured with ImageJ software via DCFH-DA. Scale bar: 100 μm. Data are presented as the mean ± SD, $n = 6$. *$P < 0.05$, **$P < 0.01$ vs the control group; #$P < 0.05$, ##$P < 0.01$ vs the PM2.5 group.

decreased in a dose-dependent manner with increasing concentrations of amygdalin up to 10 μg/mL, but increased at higher concentrations (Figure 1D). Based on the above results, pretreatment with 2.5–10 μg/mL amygdalin for 2 h before co-incubation with 100 μg/mL PM2.5 for 24 h was selected for further study.

Amygdalin attenuated PM2.5-induced oxidative stress in HUVECs

Oxidative stress is commonly regarded as one of the main hazards resulted from exposure to PM2.5. Endogenous antioxidants, such as SOD and GSH, were used to assess the ability to resist oxidative stress. As shown in Figure 2A,B, compared with those in the control group, the levels of SOD and GSH were significantly decreased in the PM2.5-exposed group, whereas amygdalin reversed these phenomena. MDA is considered as a target to measure the severity of oxidative stress. As shown in Figure 2C, PM2.5 increased MDA content in HUVECs. With the incubation of amygdalin (5 or 10 μg/mL) for 2 h before exposure to PM2.5, MDA content was significantly decreased ($P < 0.05$). These results suggested that amygdalin might protect against PM2.5-induced HUVEC injury by attenuating oxidative stress.

Amygdalin suppressed PM2.5-induced synthesis and secretion of proinflammatory cytokines and mediators in HUVECs

To investigate the anti-inflammatory effect of amygdalin, the levels of IL-6, TNF-α, IL-1β and COX-2 were examined. As shown in Figure 3A–F, the synthesis and secretion of IL-6, TNF-α and IL-1β were significantly decreased in the amygdalin-pretreated groups compared with the PM2.5 group. Additionally, after treatment with 100 μg/mL PM2.5, the relative mRNA expression of COX-2 was markedly increased compared with that in the control group (Figure 3H). Simultaneously, in the amygdalin (2.5, 5, and 10 μg/mL) pretreatment groups, a significant decrease was observed in COX-2 mRNA expression ($P < 0.01$). These results suggested that amygdalin pretreatment in a specific concentration range could effectively inhibit PM2.5-induced expressions of proinflammatory cytokines and mediators.

Amygdalin suppressed PM2.5-induced activation of the TLR4/NF-κB signaling pathway and nuclear translocation of NF-κB p65 in HUVECs

To further elucidate the anti-inflammatory mechanism of amygdalin, we quantified the levels of proteins related to the TLR4/NF-κB
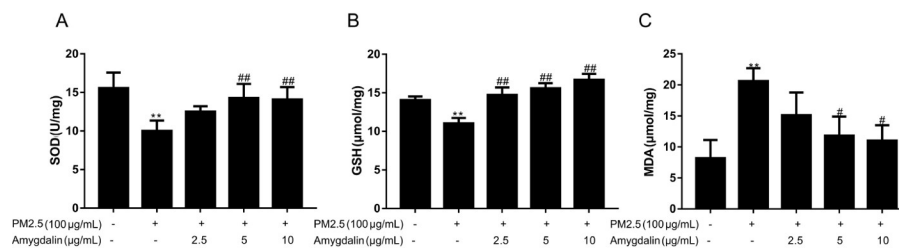

Figure 2. Protective effects of amygdalin on PM2.5-induced oxidative stress in HUVECs   HUVECs were pretreated with amygdalin (2.5, 5, and 10 μg/mL) followed by PM2.5 treatment for 24 h. The levels of SOD (A) and GSH (B) were upregulated by amygdalin in PM2.5-treated HUVECs, while the levels of MDA (C) were downregulated. Data are presented as the mean ± SD, $n = 5$. *$P < 0.05$, **$P < 0.01$ vs the control group; #$P < 0.05$, ##$P < 0.01$ vs the PM2.5 group.
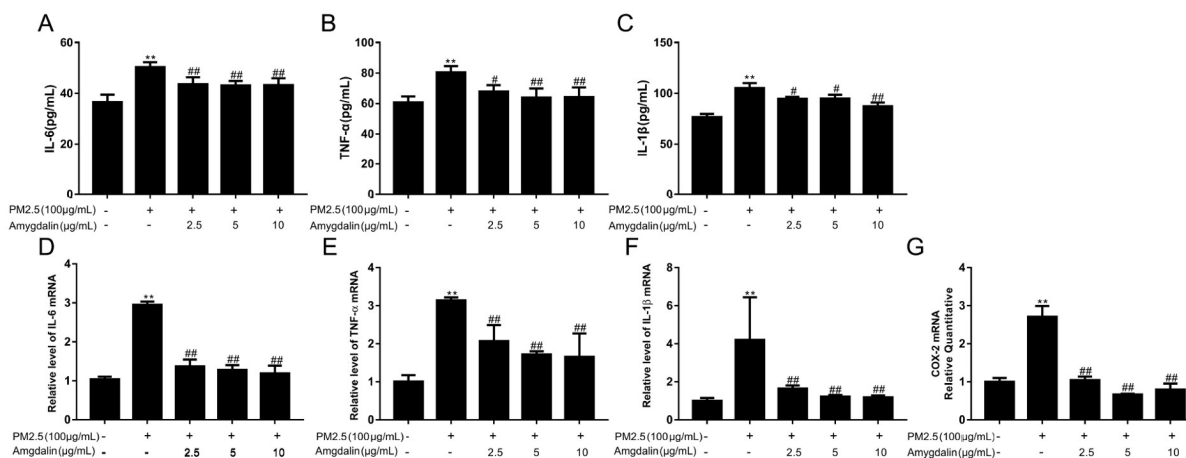

Figure 3. Effects of amygdalin on PM2.5-induced expressions of proinflammatory indicators and mediators in HUVECs   Amygdalin decreased the levels of IL-6 (A), TNF-α (B), and IL-1β (C) in PM2.5-treated HUVECs. The mRNA expression levels of *IL-6* (D), *TNF-α* (E), *IL-1β* (F) and *COX-2* (G) in PM2.5-treated HUVECs were suppressed by amygdalin. Data are presented as the mean ± SD, $n = 6$. *$P < 0.05$, **$P < 0.01$ vs the control group; #$P < 0.05$, ##$P < 0.01$ vs the PM2.5 group.

signaling pathway. As shown in Figure 4, HUVECs incubated with PM2.5 for 24 h exhibited an absolute increase in the relative protein levels of TLR4, COX-2, p-NF-κB p65/NF-κB p65, NF-κB p50, and p-IκB-α/IκB-α ($P < 0.05$).

The nuclear translocation of NF-κB p65 participates in the NF-κB signaling pathway, which plays an essential role in inflammation [35]. We further performed immunofluorescence staining to characterize the subcellular location of NF-κB p65 in HUVECs. As shown in Figure 5, PM2.5 triggered the nuclear translocation of NF-κB p65, while amygdalin inhibited this phenomenon in a dose-dependent manner.

Amygdalin attenuated PM2.5-induced apoptosis in HUVECs

The concentration of ROS under normal physiological state maintains cell functions, while excessive ROS are reported to damage cells and trigger apoptosis [36]. Previous studies have demonstrated that increased EC apoptosis is closely related to AS [25,37]. To explore the anti-apoptotic effect of amygdalin on HUVECs, apoptosis was measured by using Annexin V-FITC/PI apoptosis detection kit and TUNEL staining assay. The flow cytometry results showed that PM2.5-induced HUVEC apoptosis was markedly increased compared to that in the control group
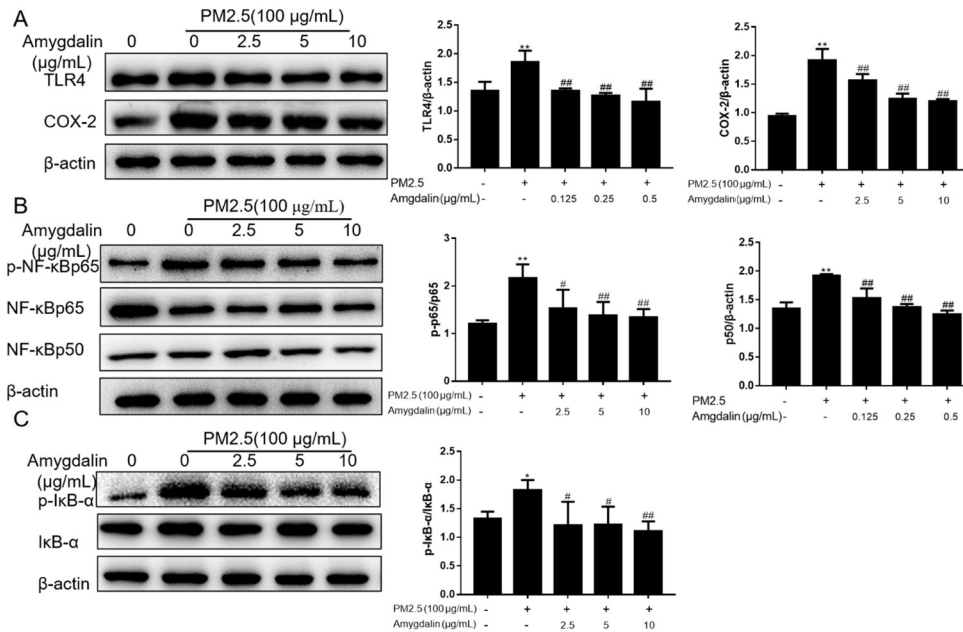

Figure 4. Amygdalin downregulated PM2.5-induced proteins related to the TLR4/NF-κB signaling pathway in HUVECs The protein expressions of TLR4 (A), COX-2 (A), p-NF-κBp65/NF-κBp65 (B), NF-κBp50 (B) and p-IκB-α/IκB-α (C) in PM2.5-treated HUVECs was inhibited by amygdalin, as revealed by western blot analysis. Quantitative analysis of protein bands was measured with ImageJ software. Data are presented as the mean ± SD, $n = 3$. *$P < 0.05$, **$P < 0.01$ vs the control group; #$P < 0.05$, ##$P < 0.01$ vs the PM2.5 group.
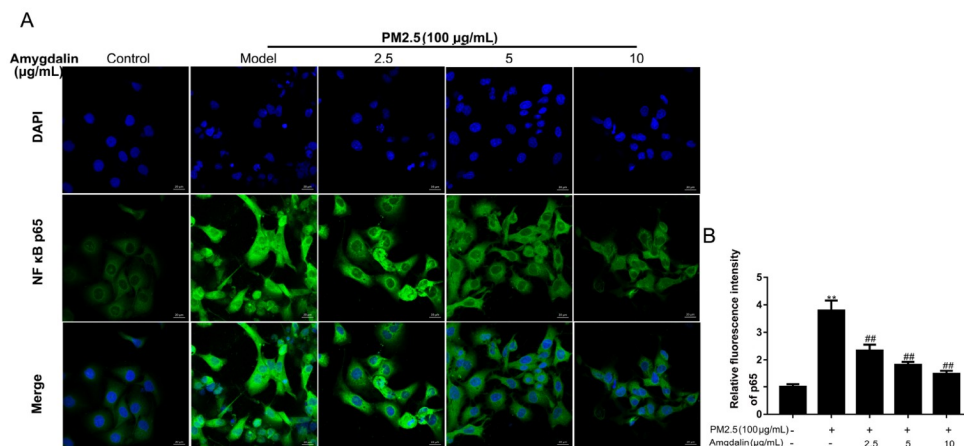

Figure 5. Amygdalin attenuated the PM2.5-induced nuclear translocation of NF-κB p65 in HUVECs Green fluorescence represents the localization of NF-κB p65, and blue fluorescence represents the nuclei of HUVECs. Scale bar: 20 μm. Data are presented as the mean ± SD, $n = 3$. *$P < 0.05$, **$P < 0.01$ vs the control group; #$P < 0.05$, ##$P < 0.01$ vs the PM2.5 group.
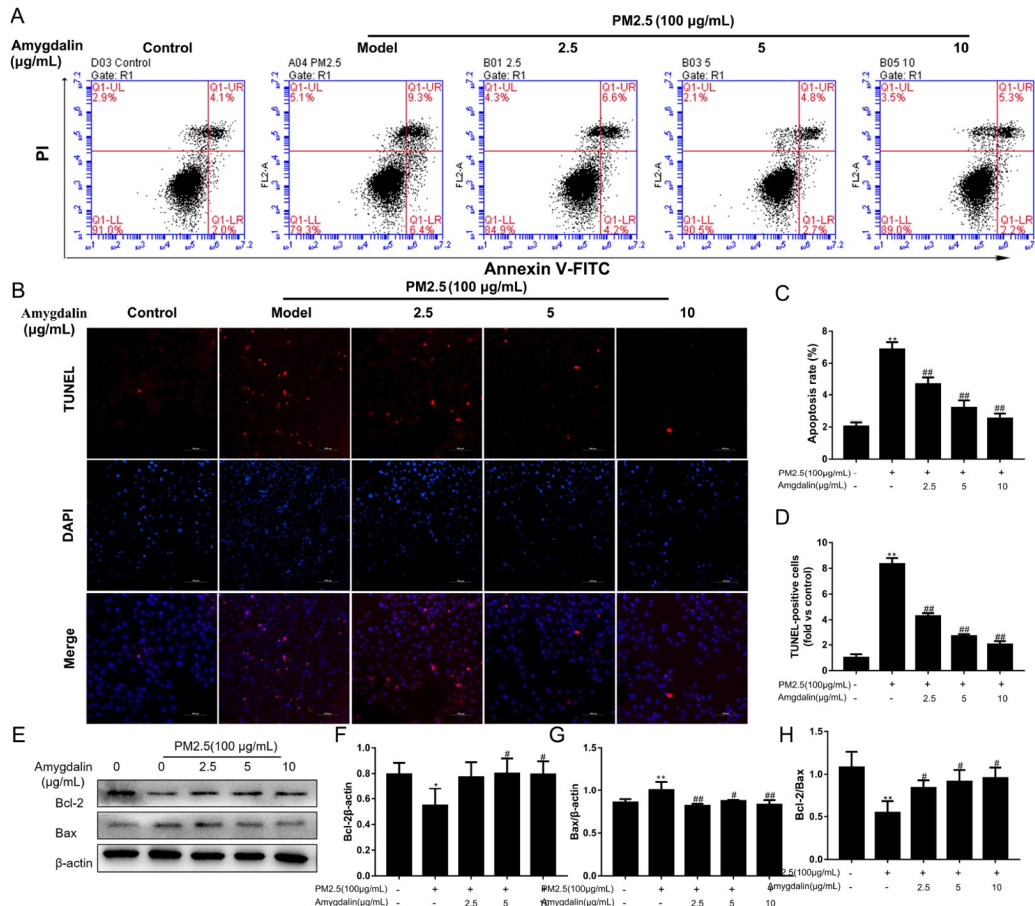
Figure 6. Amygdalin inhibited PM2.5-induced apoptosis in HUVECs (A,C) The apoptosis rate of HUVECs in each group was detected by flow cytometry. (B) Cell apoptosis detected by TUNEL staining. The red fluorescence represents TUNEL-positive cells, and the blue fluorescence represents the nuclei of HUVECs. Scale bar: 100 μm. (E) The proteins related to apoptosis (Bcl-2 and Bax) were detected by western blot analysis. (D,F,G,H) Quantitative analysis was performed with ImageJ software. Data are presented as the mean ± SD, $n = 3$. *$P < 0.05$, **$P < 0.01$ vs the control group; #$P < 0.05$, ##$P < 0.01$ vs the PM2.5 group.

(Figure 6A,C). As shown in Figure 6B,D, there were more apoptotic cells in the PM2.5 group than in the control group. In addition, a significant dose-independent decline was observed in the amygdalin-pretreated groups.

To further investigate the underlying mechanism by which amygdalin inhibits apoptosis, the proteins Bcl-2 and Bax were detected by western blot analysis. As shown in Figure 6E–H, the protein levels of Bcl-2 and Bcl-2/Bax were significantly down-regulated, and the expression of Bax was upregulated in response to PM2.5 treatment in HUVECs. In contrast, amygdalin pretreatment reversed these changes. Taken together, these findings showed that amygdalin could abrogate PM2.5-induced HUVEC apoptosis through the Bcl-2/Bax signaling pathway.

Discussion

PM2.5, the main component of haze, is closely associated with chronic inflammatory disease. According to a previous study, PM2.5 mainly causes oxidative stress, which further triggers inflammation, and apoptosis is the basic pathogenesis of AS [38,39]. A recent study showed that EC injury plays an important role in the occurrence and development of AS [25]. Earlier studies have revealed notable anti-inflammatory, anti-oxidant and anti-apoptotic effects of amygdalin. However, the role of amygdalin in

PM2.5-induced HUVEC injury has not been clarified. In the present study, we illustrated that amygdalin protected HUVECs against PM2.5-induced inflammation, oxidative stress and apoptosis through the TLR4/NF-κB and Bcl-2/Bax signaling pathways.

Recent evidence has demonstrated that PM2.5 could induce the accumulation of ROS and the imbalance of the antioxidant system, which is a major factor leading to vascular EC injury [40,41]. MDA is an oxidation product that plays an essential role in amplifying ROS and reflecting the degree of cell damage and peroxidation [42]. Intracellular antioxidants, including SOD and GSH, form the first and major line of defense against oxidative stress, which contributes to preventing toxic effects caused by ROS [19]. Previous studies have shown that PM2.5 induces EC damage and dysfunction by promoting an imbalance between ROS production and antioxidant systems, resulting in oxidative stress [17,20]. Other studies demonstrated that ameliorating oxidative stress by upregulating the levels of SOD and GSH-Px and downregulating the production of ROS and MDA could effectively alleviate HUVEC damage and dysfunction [43,44]. Our results showed that HUVECs produced low levels of ROS under normal physiological conditions. However, PM2.5 exposure intensified the accumulation of ROS. In addition, in PM2.5-treated HUVECs, the levels of SOD and GSH were significantly reduced, while the content of MDA was increased. However,

amygdalin eliminated oxidative stress damage induced by PM2.5 in HUVECs. These findings suggest that amygdalin may prevent EC dysfunction by attenuating PM2.5-induced oxidative stress.

Chronic inflammation occurs throughout the whole process of AS. Since cytokines are closely related to inflammation, regulating cytokine levels plays an essential role in the treatment of inflammatory diseases. Previous studies have illustrated that PM2.5 induces the secretion of proinflammatory cytokines and mediators, including TNF-α, IL-6, IL-1β and COX-2 [45,46]. TNF-α is regarded as a major proinflammatory cytokine, as it can promote the expression levels of multiple proinflammatory factor genes, such as *IL-6,* and amplify the inflammatory response. Moreover, a previous study showed that TNF-α is correlated with early AS [47]. IL-6, a pleiotropic cytokine, is implicated in CVD. The upregulation of IL-6 has dual effects, resulting in extravasation of leukocytes into the vessel wall and contributing to vein thrombosis [48,49]. IL-1β is one of the major members of the interleukin family, inducing the activation of neutrophils to release proinflammatory mediators. Recently, IL-1β has been considered as a potential treatment target for CVD [50]. Clinical trials utilizing canakinumab, a monoclonal antibody against IL-1β, have confirmed its significant therapeutic effect in the treatment of AS [49]. Hence, inhibition of the expressions of these pro-inflammatory cytokines may be particularly essential in the PM2.5-induced inflammatory response. Wang *et al.* [33] found that amygdalin could reduce IL-6 and TNF-α at the levels of transcription and translation in bone marrow-derived cells with the administration of ox-LDL. In the current study, we detected the levels of TNF-α, IL-6 and IL-1β to evaluate the effects of amygdalin on PM2.5-induced damage in HUVECs. As expected, amygdalin inhibited the levels of the above cytokines. In addition to inhibiting the excessive release of proinflammatory factors, amygdalin significantly downregulated TNF-α, IL-6, IL-1β and COX-2 mRNA expression levels in response to PM2.5 exposure in a dose-independent manner. These results indicate that amygdalin may alleviate HUVEC inflammation by inhibiting the secretion of proinflammatory cytokines and mediators at both the transcription and translation levels.

The TLR4/NF-κB signaling pathway widely exists in various tissues and cells, which is involved in the occurrence and regulation of cardiovascular inflammatory diseases. Previous studies illustrated that inhibiting the activation of the TLR4/NF-κB signaling pathway may be a potential strategy for the prevention and treatment of AS [51,52]. Thus, we further determined the expressions of proteins related to TLR4, COX-2 and NF-κB signaling pathways by western blot analysis. COX-2 is an inducible enzyme that is rarely expressed in normal tissues but is expressed in large quantities when inflammatory signals are transmitted to cells [53]. Our results showed that amygdalin could remarkably suppress the relative protein expression of COX-2 following PM2.5 stimulation. When pathogenic substances such as PM2.5, viruses and bacteria encounter TLR4, host pattern recognition receptors can be activated, thereby activating TLR4 and its downstream signaling molecule (NF-κB) [35,52]. In the resting state, the trimer of NF-κB binding to IκB stays in the cytoplasm. However, when extracellular stimuli are transmitted to the cytoplasm, they result in the secretion of proinflammatory cytokines and the degradation and phosphorylation of IκB protein, and subsequently lead to the activation of two subunits of NF-κB, i.e., p65 and p50 [34]. NF-κB is regarded as a crucial mediator in inflammatory and immune responses. Studies have demonstrated that activated NF-κB induces endothelial inflammation and thrombosis which plays an important role in the occurrence and development of AS [44]. Our data showed that amygdalin plays an essential role in attenuating PM2.5-induced upregulation of TLR4, NF-κB p50, p-IκB-α and p-NF-κB p65 protein expressions and nuclear translocation of NF-κB p65.

Accumulating studies have reported that the imbalance of OS promotes apoptosis. It is well known that EC apoptosis and dysfunction are the leading contributors for the pathogenesis of AS [54]. Here, we evaluated the inhibitory effects of amygdalin on PM2.5-induced apoptosis. The results indicated that amygdalin reduced EC apoptosis rate after PM2.5 administration. A previous study reported similar results that amygdalin could protect airway epithelial cells against LPS-induced apoptosis [31]. To further clarify the potential mechanism, we used western blot analysis to assess the expressions of apoptosis-related proteins. Under pathological conditions, the expression of the antiapoptotic protein Bcl-2 is inhibited, and the expression of the proapoptotic protein Bax is increased, which eventually results in accelerated apoptosis [55]. Therefore, the ratio of Bcl-2 protein to Bax protein has a crucial effect on HUVEC apoptosis. Western blot analysis showed that PM2.5 exposure upregulated the protein level of Bax and downregulated the protein levels of Bcl-2 and the Bcl-2/Bax ratio. However, amygdalin abolished these changes. These data suggest that amygdalin suppresses PM2.5-induced HUVEC apoptosis through the Bcl-2/Bax signaling pathway.

In summary, we revealed the endothelial protective effects of amygdalin on PM2.5-induced HUVEC injury, and first demonstrated that amygdalin suppresses inflammation, oxidative stress and apoptosis in response to PM2.5 in HUVECs via the TLR4/NF-κB and Bcl-2/Bax signaling pathways. Our findings suggest that amygdalin may be a potential medicine for AS treatment and lay a solid foundation for its clinical application. Further studies with specific inhibitors of suppressing the activation of TLR4/NF-κB and upregulating Bcl-2/Bax signaling pathways or overexpressing TLR4 *in vitro*, as well as *in vivo* experiments are needed to verify these findings.

Conflict of Interest
The authors declare that they have no conflict of interest.

References

1. Su R, Jin X, Li H, Huang L, Li Z. The mechanisms of PM2.5 and its main components penetrate into HUVEC cells and effects on cell organelles. *Chemosphere* 2020, 241: 125127

2. Shou Y, Huang Y, Zhu X, Liu C, Hu Y, Wang H. A review of the possible associations between ambient PM2.5 exposures and the development of Alzheimer's disease. *Ecotoxicol Environ Saf* 2019, 174: 344–352

3. Ding L, Sui X, Yang M, Zhang Q, Sun S, Zhu F, Cheng H, et al. Toxicity of cooking oil fume derived particulate matter: vitamin D3 protects tubule

formation activation in human umbilical vein endothelial cells. *Ecotoxicol Environ Saf* 2020, 188: 109905

4. Li D, Zhang R, Cui L, Chu C, Zhang H, Sun H, Luo J, *et al.* Multiple organ injury in male C57BL/6J mice exposed to ambient particulate matter in a real-ambient PM exposure system in Shijiazhuang, China. *Environ Pollution* 2019, 248: 874–887

5. Tang J, Cheng W, Gao J, Li Y, Yao R, Rothman N, Lan Q, *et al.* Occupational exposure to carbon black nanoparticles increases inflammatory vascular disease risk: an implication of an ex vivo biosensor assay. *Part Fibre Toxicol* 2020, 17: 47

6. Singh P, O'Toole TE, Conklin DJ, Hill BG, Haberzettl P. Endothelial progenitor cells as critical mediators of environmental air pollution-induced cardiovascular toxicity. *Am J Physiol-Heart Circulatory Physiol* 2021, 320: H1440–H1455

7. From the American Association of Neurological Surgeons (AANS), American Society of Neuroradiology (ASNR), Cardiovascular and Interventional Radiology Society of Europe (CIRSE), Canadian Interventional Radiology Association (CIRA), Congress of Neurological Surgeons (CNS), European Society of Minimally Invasive Neurological Therapy (ESMINT), European Society of Neuroradiology (ESNR), European Stroke Organization (ESO), Society for Cardiovascular Angiography and Interventions (SCAI), Society of Interventional Radiology (SIR), Society of NeuroInterventional Surgery (SNIS), and World Stroke Organization (WSO), Sacks D, Baxter B, Campbell BCV, Carpenter JS, Cognard C, Dippel D, Eesa M, *et al.* Multisociety consensus quality improvement revised consensus statement for endovascular therapy of acute ischemic stroke. *Int J Stroke* 2018, 13: 612–632

8. Hayes RB, Lim C, Zhang Y, Cromar K, Shao Y, Reynolds HR, Silverman DT, *et al.* PM2.5 air pollution and cause-specific cardiovascular disease mortality. *Int J Epidemiol* 2020, 49: 25–35

9. Grande G, Ljungman PLS, Eneroth K, Bellander T, Rizzuto D. Association between cardiovascular disease and long-term exposure to air pollution with the risk of dementia. *JAMA Neurol* 2020, 77: 801–809

10. Zhao D, Liu J, Wang M, Zhang X, Zhou M. Epidemiology of cardiovascular disease in China: current features and implications. *Nat Rev Cardiol* 2019, 16: 203–212

11. Zhang Y, Ji X, Ku T, Li G, Sang N. Heavy metals bound to fine particulate matter from northern China induce season-dependent health risks: a study based on myocardial toxicity. *Environ Pollution* 2016, 216: 380–390

12. Wen Y, Xiao H, Liu Y, Yang Y, Wang Y, Xu S, Huang S, *et al.* Polysaccharides from *Dendrobium officinale* ameliorate colitis-induced lung injury via inhibiting inflammation and oxidative stress. *Chemico-Biol Interactions* 2021, 347: 109615

13. Zhu X, Zhao P, Lu Y, Huo L, Bai M, Yu F, Tie Y. Potential injurious effects of the fine particulate PM2.5 on the progression of atherosclerosis in apoE-deficient mice by activating platelets and leukocytes. *Arch Med Sci* 2019, 15: 250–261

14. Wang G, Zheng X, Duan H, Dai Y, Niu Y, Gao J, Chang Z, *et al.* High-content analysis of particulate matters-induced oxidative stress and organelle dysfunction *in vitro. Toxicol In Vitro* 2019, 59: 263–274

15. Zhou FM, Chen YC, Jin CY, Qian CD, Zhu BQ, Zhou Y, Ding ZS, *et al.* Polysaccharide isolated from tetrastigma hemsleyanum activates TLR4 in macrophage cell lines and enhances immune responses in OVA-immunized and LLC-bearing mouse models. *Front Pharmacol* 2021, 12: 609059

16. Wang Y, Tang M. PM2.5 induces autophagy and apoptosis through endoplasmic reticulum stress in human endothelial cells. *Sci Total Environ* 2020, 710: 136397

17. Hu T, Zhu P, Liu Y, Zhu H, Geng J, Wang B, Yuan G, *et al.* PM2.5 induces

18. endothelial dysfunction via activating NLRP3 inflammasome. *Environ Toxicol* 2021, 36: 1886–1893

18. Yang GZ, Wang ZJ, Bai F, Qin XJ, Cao J, Lv JY, Zhang MS. Epigallocatechin-3-gallate protects huvecs from PM2.5-induced oxidative stress injury by activating critical antioxidant pathways. *Molecules* 2015, 20: 6626–6639

19. Wang L, Xu J, Liu H, Li J, Hao H. PM2.5 inhibits SOD1 expression by up-regulating microRNA-206 and promotes ROS accumulation and disease progression in asthmatic mice. *Int ImmunoPharmacol* 2019, 76: 105871

20. Guan L, Geng X, Stone C, Cosky EEP, Ji Y, Du H, Zhang K, *et al.* PM$_{2.5}$ exposure induces systemic inflammation and oxidative stress in an intracranial atherosclerosis rat model. *Environ Toxicol* 2019, 34: 530–538

21. Liu X, Lu B, Fu J, Zhu X, Song E, Song Y. Amorphous silica nanoparticles induce inflammation via activation of NLRP3 inflammasome and HMGB1/TLR4/MYD88/NF-kb signaling pathway in HUVEC cells. *J Hazard Mater* 2021, 404: 124050

22. Zhang M, Xue Y, Chen H, Meng L, Chen B, Gong H, Zhao Y, *et al.* Resveratrol inhibits MMP3 and MMP9 expression and secretion by suppressing TLR4/NF-kappaB/STAT3 activation in Ox-LDL-treated HUVECs. *Oxid Med Cell Longev* 2019, 2019: 1–15

23. Guo F, Tang C, Li Y, Liu Y, Lv P, Wang W, Mu Y. The interplay of Lnc RNA ANRIL and miR-181b on the inflammation-relevant coronary artery disease through mediating NF-κB signalling pathway. *J Cell Mol Med* 2018, 22: 5062–5075

24. Wang R, Wang W, Ao L, Wang Z, Hao X, Zhang H. Benzo[a]pyrene-7,8-diol-9,10-epoxide suppresses the migration and invasion of human extravillous trophoblast HTR-8/SVneo cells by down-regulating MMP2 through inhibition of FAK/SRC/PI3K/AKT pathway. *Toxicology* 2017, 386: 72–83

25. Bian W, Jing X, Yang Z, Shi Z, Chen R, Xu A, Wang N, *et al.* Downregulation of LncRNA NORAD promotes Ox-LDL-induced vascular endothelial cell injury and atherosclerosis. *Aging* 2020, 12: 6385–6400

26. Zhu Y, Tchkonia T, Fuhrmann-Stroissnigg H, Dai HM, Ling YY, Stout MB, Pirtskhalava T, *et al.* Identification of a novel senolytic agent, navitoclax, targeting the Bcl-2 family of anti-apoptotic factors. *Aging Cell* 2016, 15: 428–435

27. Hosny S, Sahyon H, Youssef M, Negm A. *Prunus armeniaca* L. seed extract and its amygdalin containing fraction induced mitochondrial-mediated apoptosis and autophagy in liver carcinogenesis. *ACAMC* 2021, 21: 621–629

28. Lee HM, Moon A. Amygdalin regulates apoptosis and adhesion in Hs578T triple-negative breast cancer cells. *Biomolecules Ther* 2016, 24: 62–66

29. Makarević J, Tsaur I, Juengel E, Borgmann H, Nelson K, Thomas C, Bartsch G, *et al.* Amygdalin delays cell cycle progression and blocks growth of prostate cancer cells *in vitro. Life Sci* 2016, 147: 137–142

30. Wang R, Zhang D, Tang D, Sun K, Peng J, Zhu W, Yin S, *et al.* Amygdalin inhibits TGFβ1-induced activation of hepatic stellate cells (HSCs) *in vitro* and CCl4-induced hepatic fibrosis in rats *in vivo. Int ImmunoPharmacol* 2021, 90: 107151

31. Si Z, Zhang B. Amygdalin attenuates airway epithelium apoptosis, inflammation, and epithelial-mesenchymal transition through restraining the TLR4/NF-kappaB signaling pathway on lps-treated BEAS-2B bronchial epithelial cells. *Int Arch Allergy Immunol* 2021, 182: 997–1007

32. Kung YL, Lu CY, Badrealam KF, Kuo WW, Shibu MA, Day CH, Chen RJ, *et al.* Cardioprotective potential of amygdalin against angiotensinII induced cardiac hypertrophy, oxidative stress and inflammatory responses through modulation of Nrf2 and NF-κB activation. *Environ Toxicol* 2021, 36: 926–934

33. Wang Y, Jia Q, Zhang Y, Wei J, Liu P. Amygdalin attenuates

atherosclerosis and plays an anti-inflammatory role in ApoE knock-out mice and bone marrow-derived macrophages. *Front Pharmacol* 2020, 11: 590929

34. Fu H, Liu X, Li W, Zu Y, Zhou F, Shou Q, Ding Z. PM2.5 exposure induces inflammatory response in macrophages via the TLR4/COX-2/NF-κB pathway. *Inflammation* 2020, 43: 1948–1958

35. Huang CY, Deng JS, Huang WC, Jiang WP, Huang GJ. Attenuation of lipopolysaccharide-induced acute lung injury by hispolon in mice, through regulating the TLR4/PI3K/Akt/mTOR and Keap1/Nrf2/HO-1 pathways, and suppressing oxidative stress-mediated ER stress-induced apoptosis and autophagy. *Nutrients* 2020, 12: 1742

36. Kang R, Li R, Dai P, Li Z, Li Y, Li C. Deoxynivalenol induced apoptosis and inflammation of IPEC-J2 cells by promoting ROS production. *Environ Pollution* 2019, 251: 689–698

37. Zhao H, Liu M, Liu H, Suo R, Lu C. Naringin protects endothelial cells from apoptosis and inflammation by regulating the Hippo-YAP pathway. *Biosci Rep* 2020, 40

38. Wu MY, Li CJ, Hou MF, Chu PY. New insights into the role of inflammation in the pathogenesis of atherosclerosis. *Int J Mol Sci* 2017, 18: 2034

39. Yuan T, Yang T, Chen H, Fu D, Hu Y, Wang J, Yuan Q, *et al.* New insights into oxidative stress and inflammation during diabetes mellitus-accelerated atherosclerosis. *Redox Biol* 2019, 20: 247–260

40. Xu X, Xu H, Qimuge A, Liu S, Wang H, Hu M, Song L. MAPK/AP-1 pathway activation mediates AT1R upregulation and vascular endothelial cells dysfunction under PM2.5 exposure. *Ecotoxicol Environ Saf* 2019, 170: 188–194

41. Yang S, Lian G. ROS and diseases: role in metabolism and energy supply. *Mol Cell Biochem* 2020, 467: 1–12

42. Ouyang J, Li R, Shi H, Zhong J. Curcumin protects human umbilical vein endothelial cells against H_2O_2-Induced cell injury. *Pain Res Manage* 2019, 2019: 1–7

43. Liao L, Gong L, Zhou M, Xue X, Li Y, Peng C. Leonurine ameliorates oxidative stress and insufficient angiogenesis by regulating the PI3K/Akt-eNOS signaling pathway in H_2O_2-induced HUVECs. *Oxid Med Cell Longev* 2021, 2021: 1–12

44. Hu R, Wang MQ, Ni SH, Wang M, Liu LY, You HY, Wu XH, *et al.* Salidroside ameliorates endothelial inflammation and oxidative stress by regulating the AMPK/NF-κB/NLRP3 signaling pathway in AGEs-induced HUVECs. *Eur J Pharmacol* 2020, 867: 172797

45. Chenxu G, Minxuan X, Yuting Q, Tingting G, Jinxiao L, Mingxing W, Sujun W, *et al.* iRhom2 loss alleviates renal injury in long-term PM2.5-exposed mice by suppression of inflammation and oxidative stress. *Redox Biol* 2018, 19: 147–157

46. Kim RE, Shin CY, Han SH, Kwon KJ. Astaxanthin suppresses PM2.5-induced neuroinflammation by regulating Akt phosphorylation in BV-2 microglial cells. *Int J Mol Sci* 2020, 21: 7227

47. Kojima Y, Volkmer JP, McKenna K, Civelek M, Lusis AJ, Miller CL, Direnzo D, *et al.* CD47-blocking antibodies restore phagocytosis and prevent atherosclerosis. *Nature* 2016, 536: 86–90

48. Zhang Y, Zhang Z, Wei R, Miao X, Sun S, Liang G, Chu C, *et al.* IL (interleukin)-6 contributes to deep vein thrombosis and is negatively regulated by miR-338-5p. *Arterioscler Thromb Vasc Biol* 2020, 40: 323–334

49. Ridker PM, Everett BM, Thuren T, MacFadyen JG, Chang WH, Ballantyne C, Fonseca F, *et al.* Antiinflammatory therapy with canakinumab for atherosclerotic disease. *N Engl J Med* 2017, 377: 1119–1131

50. Abbate A, Toldo S, Marchetti C, Kron J, Van Tassell BW, Dinarello CA. Interleukin-1 and the inflammasome as therapeutic targets in cardiovascular disease. *Circ Res* 2020, 126: 1260–1280

51. Pei X, Wen Y, Cui F, Yang Z, Xie Z. lncRNA CASC7 regulates pathological progression of ox-LDL-stimulated atherosclerotic cell models via sponging miR-21 and regulating PI3K/Akt and TLR4/NF-κB signaling pathways. *Aging* 2021, 13: 25408–25425

52. Liang X, Xiu C, Liu M, Lin C, Chen H, Bao R, Yang S, *et al.* Platelet-neutrophil interaction aggravates vascular inflammation and promotes the progression of atherosclerosis by activating the TLR4/NF-κB pathway. *J Cell Biochem* 2019, 120: 5612–5619

53. Hashemi Goradel N, Najafi M, Salehi E, Farhood B, Mortezaee K. Cyclooxygenase-2 in cancer: a review. *J Cell Physiol* 2019, 234: 5683–5699

54. Wang Z, Zhang M, Wang Z, Guo Z, Wang Z, Chen Q. Cyanidin-3-*O*-glucoside attenuates endothelial cell dysfunction by modulating miR-204-5p/SIRT1-mediated inflammation and apoptosis. *BioFactors* 2020, 46: 803–812

55. Dong Y, Chen H, Gao J, Liu Y, Li J, Wang J. Molecular machinery and interplay of apoptosis and autophagy in coronary heart disease. *J Mol Cell Cardiol* 2019, 136: 27–41